

Article

Time-Resolved IR Spectroscopy Reveals a Mechanism with TiO₂ as a Reversible Electron Acceptor in a TiO₂ – Re Catalyst CO₂ Photoreduction System

Mohamed Abdellah, Ahmed M. El-Zohry, Liisa J. Antila, Christopher D. Windle, Erwin Reisner, and Leif Hammarström

J. Am. Chem. Soc., **Just Accepted Manuscript** • Publication Date (Web): 24 Dec 2016

Downloaded from <http://pubs.acs.org> on December 26, 2016

Just Accepted

“Just Accepted” manuscripts have been peer-reviewed and accepted for publication. They are posted online prior to technical editing, formatting for publication and author proofing. The American Chemical Society provides “Just Accepted” as a free service to the research community to expedite the dissemination of scientific material as soon as possible after acceptance. “Just Accepted” manuscripts appear in full in PDF format accompanied by an HTML abstract. “Just Accepted” manuscripts have been fully peer reviewed, but should not be considered the official version of record. They are accessible to all readers and citable by the Digital Object Identifier (DOI®). “Just Accepted” is an optional service offered to authors. Therefore, the “Just Accepted” Web site may not include all articles that will be published in the journal. After a manuscript is technically edited and formatted, it will be removed from the “Just Accepted” Web site and published as an ASAP article. Note that technical editing may introduce minor changes to the manuscript text and/or graphics which could affect content, and all legal disclaimers and ethical guidelines that apply to the journal pertain. ACS cannot be held responsible for errors or consequences arising from the use of information contained in these “Just Accepted” manuscripts.



ACS Publications

Time-Resolved IR Spectroscopy Reveals a Mechanism with TiO₂ as a Reversible Electron Acceptor in a TiO₂—Re catalyst CO₂ Photoreduction System

Mohamed Abdellah ^{a,b,*}, Ahmed M. El-Zohry ^a, Liisa J. Antila ^a, Christopher D. Windle ^c,
Erwin Reisner ^c, and Leif Hammarström ^{a*}

^a Ångström Laboratory, Department of Chemistry, Uppsala University, Box 523, 75120 Uppsala, Sweden

^b Department of Chemistry, Qena Faculty of Science, South Valley University, 83523 Qena, Egypt

^c Christian Doppler Laboratory for Sustainable SynGas Chemistry, Department of Chemistry, University of Cambridge, Lensfield Road, Cambridge CB2 1EW, U.K.

KEYWORDS: CO₂ photo-catalytic reduction, fs and ns time resolved IR spectroscopy, TEOA, Re molecular catalyst, and photo-catalytic mechanism

ABSTRACT: Attaching the phosphonated molecular catalyst [Re^IBr(bpy)(CO)₃]⁰ to the wide-band gap semiconductor TiO₂ strongly enhances the rate of visible-light driven reduction of CO₂ to CO in dimethyl formamide (DMF) with triethanolamine (TEOA) as sacrificial electron donor. Herein, we show by transient mid-IR spectroscopy that the mechanism of catalyst photoreduction is initiated by ultrafast electron injection into TiO₂, followed by rapid (ps-ns) and sequential two-electron oxidation of TEOA that is coordinated to the Re center. The injected electrons can be stored in the conduction band (CB) of TiO₂ on a ms-s time scale, and we propose they lead to further reduction of the Re-catalyst and completion of the catalytic cycle. Thus, the excited Re catalyst gives away one electron and would eventually get three electrons back. The function of an electron reservoir would represent a role for TiO₂ in photo-catalytic CO₂ reduction that has previously not been considered. We propose that the increase in photocatalytic activity upon heterogenisation of the catalyst to TiO₂ is due to the slow charge recombination and the high oxidative power of the Re^{II} species after electron injection, as compared to the excited MLCT state of the unbound Re catalyst or when immobilized on ZrO₂, which results in a more efficient reaction with TEOA.

INTRODUCTION

Tremendous efforts have been made to explore new energy resources in order to face the problems of energy shortage and global warming. Continuous increase of the CO₂ concentration in the atmosphere is the main reason behind global warming.¹ A smart solution is to convert CO₂ emissions to fuels or other useful chemicals, which is one of the goals of artificial photosynthesis.²⁻

¹⁰ Photocatalytic and photoelectrocatalytic reduction of CO₂ has been achieved by employing metals and semiconductors¹¹⁻¹³ or enzymes bound to photoelectrodes.^{14,15} The former suffers from poor selectivity and, in contrast, the latter shows excellent selectivity but suffers from stability issues.^{14,15} Balancing between both high selectivity and stability can potentially be achieved using synthetic molecular catalyst for CO₂ reduction.^{7,10,11,16-20} Generally, there are two approaches to CO₂ photoreduction with synthetic molecular catalysts. In the first one, the catalyst receives electrons from a photosensitizer after the excitation. In the second approach, the catalyst itself plays a dual role, working as both photosensitizer and catalyst, as exemplified by the rhenium tricarbonyl bipyridine bromide [Re^IBr(bpy)(CO)₃]⁰ catalyst.^{7,20}

Recently, some of us attached this catalyst to an n-type TiO₂ semiconductor *via* phosphonic acid linker groups (TiO₂—[Re(2,2'-bipyridine-4,4'-bisphosphonic acid)(CO)₃(L)]), where initially L = Br⁻ but is replaced during the photoreaction; Scheme

1). In the presence of triethanolamine (TEOA as electron donor this led to a higher yield (TON) of CO₂ photoreduction compared to both the homogenous system without TiO₂ and to systems where the same catalyst was attached to other metal oxides, such as ZrO₂.²¹ TiO₂ was proposed to stabilize reduced catalyst intermediates and hinder formation of unreactive Re-Re dimers, but not participate directly in the electron transfer reactions.

In the present study we attempt to answer several questions, in order to understand the role of TiO₂ and to propose the photoreduction mechanism of the attached catalyst. First, is TiO₂ unreactive or is the excited [ReBr(bpy)(CO)₃] oxidized by electron injection into TiO₂ as has been shown in some cases²²? Second, what are the roles of the TEOA in the photocatalytic process? Finally, what is the role of TiO₂ in the photoreduction process? To answer these questions we used time-resolved IR (TRIR) in the region of CO stretching vibrations, from time scales of femtosecond up to seconds. The ν(CO) is very sensitive to the electron density of the central Re ion, allowing us to identify and follow the Re excited state and different oxidation states.²³⁻²⁵

EXPERIMENTAL SECTION

Steady-state spectroscopy. Steady-state absorption and emission were recorded using a Varian Cary 5000 and a Horiba Jobin Yvon Fluorolog, respectively. The emission spectrum for

[Re^IBr(bpy)(CO)₃]⁰ in DMF was corrected for the wavelength-dependent instrument sensitivity and measured at the right angle using 1 cm quartz cuvette. IR spectrum for [Re^IBr(bpy)(CO)₃]⁰ in DMF was recorded in a modified Omni cell (Specac) with O-ring sealed CaF₂ windows and a path length of 100 μm using a Bruker IFS 66v/S FTIR spectrophotometer controlled by OPUS software. IR spectra for TiO₂—[Re^I(bpy)(CO)₃DMF]⁺ on CaF₂ films were measured directly using the same setup. In order to monitor the ligand exchange in the presence of TEOA and CO₂, the attached catalyst on TiO₂ films (on CaF₂) were immersed into a DMF/TEOA (5:1) mixture with continuous CO₂ bubbling.

Ultrafast transient mid-IR absorption spectroscopy. The 1 mJ, 45 fs output of a 1 kHz Ti:Sapphire amplifier (Spitfire Pro, Spectra-Physics) was split into two separate commercial optical para-metric amplifiers (TOPAS-C, Light Conversion), which generate the visible pump 418 nm and the mid-IR probe (1850–2200 cm⁻¹) pulses. Prior to reaching the sample, the probe beam was split into equal intensity probe and reference beams using a wedged ZnSe window. Both beams pass through the sample, but only the probe beam interacts with the photoexcited volume of the sample. All beams are focused with a single f = 10 cm off axis parabolic mirror to a ~70 μm spot size in the sample. The pump intensity was attenuated to 650 μW. The probe and reference beams were dispersed by a commercial monochromator (Triax 190, HORIBA Jobin Yvon) equipped with a 75 groove/mm grating and detected on a dual array, 2x64 pixel mercury cadmium telluride detector (InfraRed Associated, Inc). The instrument response function for the experiments was approximately 100 fs. The sample was mounted in a Harrick flow cell.²⁶

Transient mid-IR absorption spectroscopy. A frequency doubled Q-switched Nd:YAG laser (Quanta-Ray ProSeries, Spectra-Physics) was employed to obtain 355 nm pump light, 10 mJ/pulse with a FWHM of 10 ns. 355 nm pump light used through MOPO crystal to generate 440 nm light to pump the sample. Probing was done with the continuous wave quantum cascade (QC) IR laser with a tuning capability between 1960–2150 cm⁻¹ (Daylight Solutions). For IR detection a liquid nitrogen-cooled mercury cadmium telluride (MCT) detector (KMPV10-1-J2, Kolmar Technologies, Inc.) was used. The IR probe light was overlapped with the pump beam in a quasi-co-linear arrangement at 25° angle. Transient absorption traces were acquired with a Tektronix TDS 3052 500 MHz (5GS/s) oscilloscope in connection with the L900 software (Edinburgh Instruments) and processed using Origin 9 software.^{27,28}

For the spectroscopy measurements, 2 mg of the catalyst is dissolved in 10 ml of DMF then mesoporous TiO₂ (anatase nanoparticles with average size ~ 20 nm and bandgap ~3.2 eV) films are immersed in this solution for the sensitization process for 20 hours while the photo-catalytic measurements carried out for colloidal TiO₂—catalyst hybrid system.²¹ The catalyst has a broad MLCT band at λ = 380 nm followed by a ultra-violet band below 352 nm due to ligand centered transitions.²⁹ The MLCT band maintains the same after the attachment to the TiO₂ (Figure S1B).²⁴ The MLCT state generates a characteristic broad emission band at λ = 600 nm for the triplet state ³(Re)* (see inset of Figure S1B). The FTIR spectrum for TiO₂—[Re^I(bpy)(CO)₃DMF] shows the stretching vibration of the (CO)₃ groups at 2041 and 1934 cm⁻¹ which confirms i) the attachment of the catalyst on TiO₂ surface. And ii) the replacement of the Br ligand with DMF ligand on the surface of TiO₂ (Figure S1C). The stretching vibration of the (CO)₃ groups shifts from 2024 and 1882 cm⁻¹ for the Br version to higher wavenumbers due to the formation of DMF version.^{21,30}

RESULTS AND DISCUSSION

Electron injection from excited [Re^I(bpy)(CO)₃DMF]* to TiO₂: To investigate the electron injection from the excited catalyst [Re^I(bpy)(CO)₃DMF]* to TiO₂, first we used the same sensitization conditions to attach the catalyst to ZrO₂ (non-injecting semiconductor as a reference).³¹ Then we used fs-TRIR to test the electron injection process. The ZrO₂—[Re^I(bpy)(CO)₃DMF]⁺ system shows the typical spectral features of the excited [Re^I(bpy)(CO)₃]*: the bleach of the ground state CO bands (GSB) at ~2040 cm⁻¹ and around 1960 cm⁻¹ and the corresponding excited-state bands (ESA) at ~2057 cm⁻¹ and around 2010 cm⁻¹ (Figure 1A).³² In addition to these spectral features, the TiO₂—[Re^I(bpy)(CO)₃DMF]⁺ system shows: i) a new peak on the higher wavenumber side compared to the ground state bleach (GSB) due to the oxidized state of the catalyst, [Re^{II}(bpy)(CO)₃DMF]²⁺ (at 2088 cm⁻¹)²⁵ ii) a broad absorption band in the entire probe region due to electrons in the TiO₂ conduction band (CB) (TiO₂(e⁻)—[Re^{II}(bpy)(CO)₃DMF]²⁺)^{22,25} (Figure 1B). The amplitude of both the oxidized catalyst [Re^{II}(bpy)(CO)₃]²⁺ peak and the electrons in the TiO₂ CB increase with increasing delay time with no decay up to 5 ns. Thus, there is no observable charge recombination on this time scale, but instead a slow additional component of electron injection. The traces at 2088 cm⁻¹ (oxidized catalyst after back ground subtraction of e⁻_{CB} signal) and at 2125 cm⁻¹ (e⁻_{CB} signal) have different kinetics (Figure S2B). The electron trace shows significant appearance of the e⁻_{CB} signal on a ~2 ps time scale, while the oxidized catalyst peak growth is slower (~30 ps). This difference could be because the electron signal is very strong and initially buries the oxidized catalyst peak. The catalyst peak is initially broad but narrows with time, and is thus more clearly seen, as has been observed before.^{22,32,33} The spectral narrowing occurs on ~30 ps time scale. In separate experiments using ns-laser excitation with a cw-IR laser probe (see Experimental section), we found that the electrons recombine on the tens of μs time scale (Figure S2A).

The role of TEOA: TEOA is not just an external (outer-sphere) electron donor in DMF solutions. Instead, under illumination in the presence of TEOA the [Re^I(bpy)(CO)₃DMF]⁺ catalyst binds CO₂ in the form of a TEOA-CO₂ carbonate ligand ([Re^I(bpy)(CO)₃-OC(O)O-(CH₂)₂NR₂)⁰; Scheme 1). Ishitani and coworkers showed the analogous ligand exchange process for the homogeneous [Re^I(bpy)(CO)₃DMF]⁺ catalyst in the presence of TEOA and CO₂ by using FTIR and ESI-MS measurements.³⁰ Based on their findings and FTIR spectra, we could confirm the formation of TiO₂—[Re^I(bpy)(CO)₃-OC(O)O-(CH₂)₂NR₂)⁰ under irradiation in the presence of TEOA and CO₂ (Figure S3A, S3C and scheme 1). Fs-TRIR spectroscopy shows that also after ligand exchange the new species [Re^I(bpy)(CO)₃-OC(O)O-(CH₂)₂NR₂)⁰ is able to inject electrons to TiO₂ (Figure S3B and S3D). The ultrafast electron injection has the same amplitude with and without TEOA and CO₂ indicating that the injecting species is the major species (Figure S3E).

Moreover, we found that for TiO₂—[Re^I(bpy)(CO)₃-OC(O)O-(CH₂)₂NR₂)⁰ the oxidized catalyst TRIR peak on the high wavenumber side of the GSB is absent, while the electrons are clearly present in the CB of TiO₂. Thus, the TEOA-ligand seems to be able to reduce the oxidized catalyst on the same time scale as the electron injection process, forming the species where the “hole” has moved to the TEOA ligand: TiO₂(e⁻)—[Re^I(bpy)(CO)₃-OC(O)O-(CH₂)₂N⁺R₂)⁺. Figure 1C shows the TRIR spectra of TiO₂—[Re^I(bpy)(CO)₃-OC(O)O-(CH₂)₂NR₂)⁰ where the e⁻_{CB} signal at 2100 cm⁻¹ has been subtracted, to emphasize the molecular signals. The CO signals of TiO₂(e⁻)—[Re^I(bpy)(CO)₃-OC(O)O-(CH₂)₂N⁺R₂)⁺ are upshifted compared to the ground state complex, consistent with formation of a cation radical in the vicinity of the Re^I center. We note that the spectra

are similar to those of the (bpy)Re^{II} MLCT state on ZrO₂, but they are more narrow and do not show the same shift with time as the MLCT state on ZrO₂. For TiO₂ sample the peak stabilizes at 2036±1 cm⁻¹ within 1 ps while the ZrO₂ sample red-shifts by 10 cm⁻¹ during 500 ps (see Figure S4). The signal of TiO₂(e⁻)—[Re^I(bpy)(CO)₃OC(O)O-(CH₂)₂N⁺R₂]⁺ should therefore not be mistaken for an MLCT state.

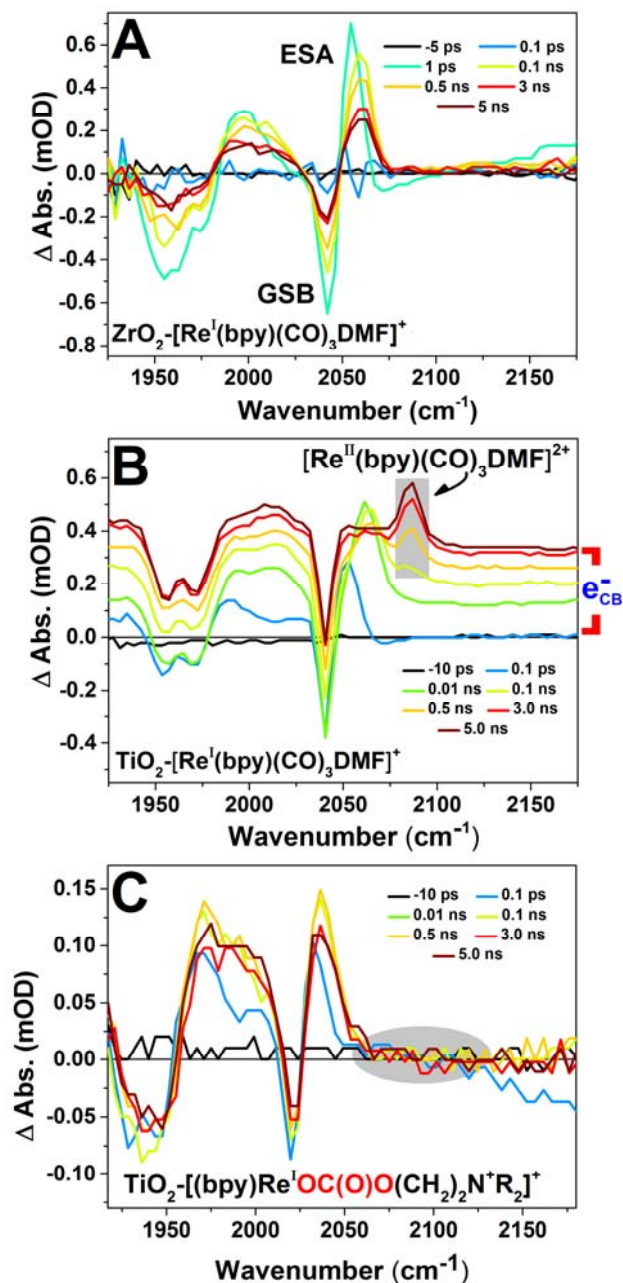
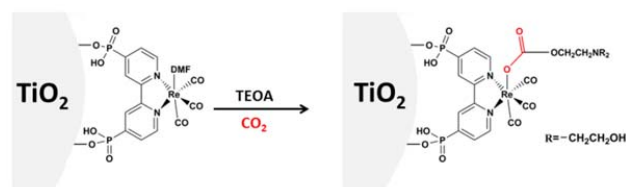


Figure 1, A) fs-TRIR for the ZrO₂—[Re^I(bpy)(CO)₃]⁺ system in DMF, B) fs-TRIR for the TiO₂—[Re^I(bpy)(CO)₃]⁺ system without TEOA, and C) fs-TRIR for the TiO₂—[Re^I(bpy)(CO)₃OC(O)O-(CH₂)₂N⁺R₂]⁺ system in DMF/TEOA solution (5:1) and CO₂ bubbling (the absorption at 2100 cm⁻¹ was subtracted from the spectra to emphasize molecular signals).



Scheme 1. Ligand exchange process combined with CO₂ capturing of the [Re^I(bpy)(CO)₃DMF]⁺ catalyst in TEOA/CO₂ solution.

The reactions were followed on a longer time scale using a ns-laser/TRIR setup. Figure 2 compared the TRIR spectra of TiO₂—[Re^I(bpy)(CO)₃DMF]⁺ without (2A) and with (2B) TEOA and CO₂. At first sight, in figure 2A, we can recognize the GSB peak and the oxidized catalyst peak TiO₂(e⁻)—[Re^{II}(bpy)(CO)₃DMF]²⁺ on the higher wavenumber side, which agrees very well with the fs-FTIR results of Figure 1A. These signals decay on a time scale of a few μs. In contrast, after introducing TEOA and CO₂, we found that, in addition to the GSB of TiO₂(e⁻)—[Re^I(bpy)(CO)₃OC(O)O-(CH₂)₂NR₂]^{0/30} at 2020 cm⁻¹, an absorption peak appears on the lower wavenumber side, and this grows stronger during the first few 100's of ns. This means an increased electron density on the Re center, and can be attributed to a singly reduced catalyst.^{34,35} Our assignment is based on the following spectral analysis. We subtract the spectrum at 50 ns from the spectrum at .org/10.1021/ic10234p</url></related-urls></urls><electronic-2 (Figure S3F). The resulting peak at 2015 cm⁻¹ for the sample with TEOA/CO₂ which is in good agreement with the results of Kubiak and coworkers,³⁴ who reported the FTIR spectrum of the singly reduced species [(ⁱbu₂-bpy)(CO)₃ReCl]⁰ (ⁱbu₂-bpy = 4,4'-di-*tert*-butyl-2,2'-bipyridine), where the added electron density centered mostly on the bipyridine ligand.³⁴ The electron density on the Re center induced by the anionic Cl⁻ ligand in their work is matched by the carbonate ligand in the present case. The doubly oxidized TEOA (R₂-N-(CH₂)₂OH) is formed *via* deprotonation and rearrangement to the corresponding R₂N⁺=CH-CH₂OC(O)O⁻ species. Thus, we propose the structural notation TiO₂(e⁻)—[Re^I(bpy)(CO)₃OC(O)O-CH₂CHN⁺R₂]⁰ for the reduced catalyst species, from which one proton has been released. Note that the formation of the singly reduced catalyst is not on the expense of the electrons in the TiO₂ CB as the entire background absorption increases on the same time scale (Figure 2B). The only other plausible electron source for catalyst reduction is the oxidized TEOA radical [OC(O)O(CH₂)₂NR₂][•] that is unstable and highly reducing, so that each TEOA can donate two equivalents of electrons.³⁶⁻³⁹ On ZrO₂ instead, there was no measurable formation of the singly reduced catalyst on this time scale (Figure S3F). This finding confirms that electron injection from [Re^I(bpy)(CO)₃OC(O)O-(CH₂)₂NR₂]⁺ into TiO₂ plays a role in the photoreduction process. This triggers the first oxidation of TEOA on a ps time scale, and releases a second equivalent of electrons on a time scale of ~1 μs. The second equivalent mostly reduces the Re catalyst, but some apparently ends up as CB electron. This can possibly be explained by the close proximity of the Re-coordinated TEOA to TiO₂, or by prior decooordination of TEOA radical from the Re complex. Thermodynamically, TEOA radical has enough reducing power to reduce Re complex and consequently, it is able to reduce the CB of TiO₂.³⁷ Figure 3A compares the traces at 2015 cm⁻¹ with and without introducing TEOA/CO₂, corresponding to the transient spectra in Figure 2, which illustrates the differences in reactions on this time scale.

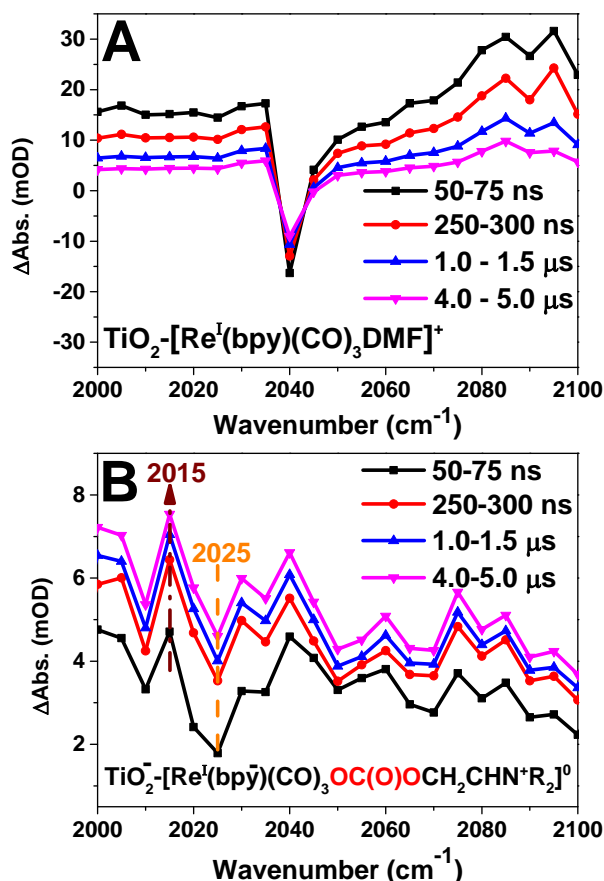


Figure 2, A) ns-TRIR spectra at different time delays after the photo-excitation for A) $\text{TiO}_2\text{--}[\text{Re}^{\text{I}}(\text{bpy})(\text{CO})_3\text{DMF}]^+$, and B) $\text{TiO}_2\text{--}[\text{Re}^{\text{I}}(\text{bpy})(\text{CO})_3]$ in the presence of TEOA/ CO_2 . The molecular GSB is at 2040 and 2025 cm^{-1} , respectively, in agreement with FTIR spectra. Panel B marks also the peak at 2015 cm^{-1} for the singly reduced catalyst $\text{TiO}_2(\text{e}^-)\text{--}[\text{Re}^{\text{I}}(\text{bpy})(\text{CO})_3\text{OC}(\text{O})\text{OCH}_2\text{CHN}^+\text{R}_2]^0$.

In the absence of TEOA/ CO_2 most of the signal from CB electrons in TiO_2 decays within 10 μs , by charge recombination with the oxidized catalyst: $\text{TiO}_2(\text{e}^-)\text{--}[\text{Re}^{\text{II}}(\text{bpy})(\text{CO})_3\text{DMF}]^{2+} \rightarrow \text{TiO}_2\text{--}[\text{Re}^{\text{I}}(\text{bpy})(\text{CO})_3\text{DMF}]^+$. In the sample with TEOA/ CO_2 instead, the electrons in the TiO_2 CB do not show any decay up to tens of ms (Figures 3A and 3B). From the transient spectra and traces it is clear that the reduced catalyst $[\text{Re}^{\text{I}}(\text{bpy})(\text{CO})_3\text{OC}(\text{O})\text{OCH}_2\text{CHN}^+\text{R}_2]^0$ forms on a rapid time scale $\tau_1 = 35$ ns followed by a slow rise in Figure 3A ($\tau_2 = 1.8$ μs). At the same time the background signal of CB electrons increases for which the IR extinction coefficient is larger than for the catalyst species (*cf.* the relative ΔAbs of the molecular peak vs. broad background in Figure 2B).

TiO_2 role in CO_2 photoreduction by $[\text{Re}^{\text{I}}(\text{bpy})(\text{CO})_3]^+$ catalyst: The data indicate that there is an electron injection from the excited $[\text{Re}^{\text{I}}(\text{bpy})(\text{CO})_3\text{L}]^*$ to the TiO_2 CB on the ps time scale. For the sample with TEOA/ CO_2 this leads to phototriggered oxidation of TEOA and formation of a reduced catalyst, which is not seen on ZrO_2 . Therefore, TiO_2 has an active role in the light induced electron transfer reactions of this system. To further investigate the role of TiO_2 we probed the destiny of CB electrons on longer time scales.

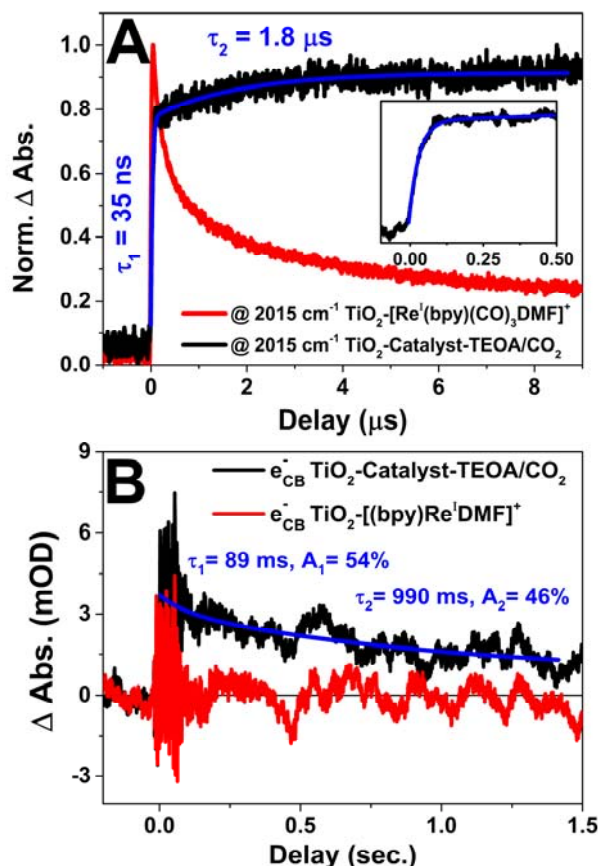


Figure 3, A) traces at 2015 cm^{-1} for TiO_2 -catalyst (red) and for TiO_2 -catalyst in the presence of TEOA and CO_2 (black) up to 10 μs (inset: showing the rising component), and B) traces at 2100 cm^{-1} (electrons in the TiO_2 CB) for TiO_2 -catalyst (red) and TiO_2 -catalyst in the presence of TEOA/ CO_2 (black) up to 1.5 sec. delay after the photo-excitation.

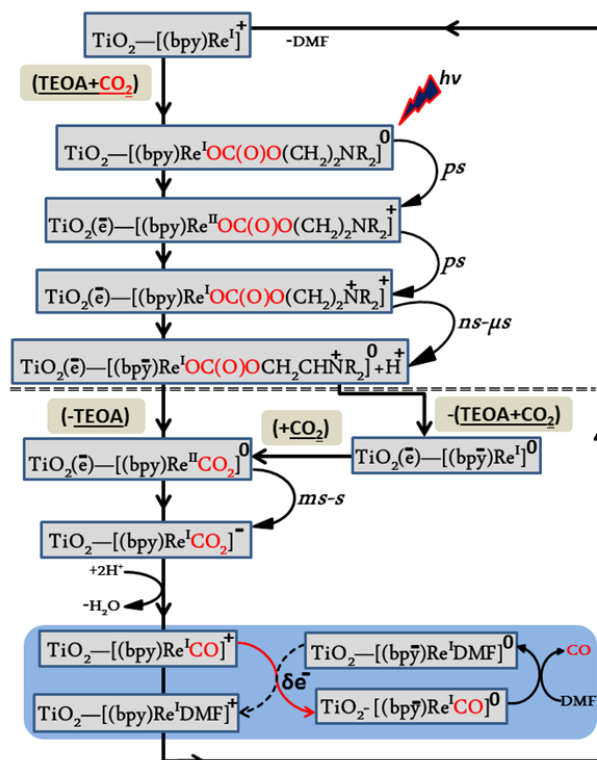
Figure 3B compares the traces at 2100 cm^{-1} (CB electron absorption region) up to 1.5 seconds after photo-excitation of the TiO_2 -catalyst without (red trace) and with introducing TEOA/ CO_2 (black trace). Without TEOA/ CO_2 no electrons are left in the TiO_2 CB on this time scale, but introduction of TEOA and CO_2 to the attached catalyst changes the kinetics drastically. Clearly, the electrons are still in the TiO_2 CB on this time scale and only around 50% of the electrons had disappeared from the CB after around 100 ms, while the remaining 50% decays with $\tau \sim 1$ s. This time scale ($\tau \sim 1$ s) is very similar to what was reported for decay of the reduced catalyst signal ($\tau = 0.4$ s) at 500 nm (bpyRe^{I} - signal)²¹ even though we could not follow the molecular signal by mid IR on the ms to seconds time scale. It is important to note that there is no accumulation of more reduced catalyst species upon repeated laser flashing or continuous irradiation. Thus, we propose that the CB electrons are added to the reduced catalyst, and lead to catalytic turnover, restoring the sample to the initial $\text{TiO}_2\text{--}[\text{Re}^{\text{I}}(\text{bpy})(\text{CO})_3\text{OC}(\text{O})\text{O}(\text{CH}_2)_2\text{NR}_2]^0$ state; we discuss a possible mechanism in the next section. At present we do not know if the CB electrons that decay with $\tau \sim 89$ ms also contribute to catalyst reduction, or if they are lost in side reactions. In any case, these experiments add more evidence that TiO_2 plays a role in the photocatalytic reduction of CO_2 in this system other than being a scaffold. In this context, we note again that formation of the singly reduced catalyst $[\text{Re}^{\text{I}}(\text{bpy})(\text{CO})_3\text{--}$

OC(O)O-(CH₂)₂N⁺R₂)⁰ on ZrO₂, by quenching of the excited Re complex by the appended TEOA, was not measurable (Figure S3F), which means that the electron injection process in TiO₂ promotes formation of this species. This agrees well with the differences in catalytic activity of the catalyst on TiO₂ and on ZrO₂.²¹

Proposed photocatalytic mechanism: The mechanism of CO₂ reduction by [Re^I(bpy)(CO)₃L] catalysts is still under debate, with different mechanistic pathways being discussed.^{8,35,40,41} Under electro-catalytic reduction conditions, the complex typically undergoes a two-electron reduction and loses the labile ligand (L) to form a [Re(bpy)(CO)₃]⁻ species that binds to CO₂ and enters the catalytic cycle.⁴¹ However, under photo-catalytic reduction conditions, already the one-electron-reduced complex [Re⁰(bpy)(CO)₃] may bind to CO₂ and start the catalytic cycle.⁴² Attaching the catalyst to TiO₂, improves the catalytic activity but it also increases the mechanistic complexity further. Scheme 2 presents our proposed mechanism of the photo-catalytic reduction of CO₂ using TiO₂-[Re^I(bpy)(CO)₃DMF]⁺ system in the presence of TEOA/CO₂ in DMF solution. As shown above TiO₂-[Re^I(bpy)(CO)₃]⁺ is able to capture CO₂ and bind it as a carbonated TEOA ligand, forming the catalyst TiO₂-[Re^I(bpy)(CO)₃-OC(O)O-(CH₂)₂NR₂]⁰. Upon photoexcitation of this complex, electron injection into the CB of TiO₂ occurs on the ps time scale. This is rapidly followed by electron transfer from the bound TEOA ligand [-CH₂)₂NR₂] to the oxidized catalyst to form TiO₂(e⁻)-[Re^{II}(bpy)(CO)₃-OC(O)O-(CH₂)₂N⁺R₂]⁺. On a ns-μs time scale the (-CH₂)₂NR₂)⁺ radical cation shifts the radical from the nitrogen to an adjacent carbon, that deprotonates, and donates a second electron to further reduce the complex and form TiO₂(e⁻)-[Re^I(bpy)(CO)₃-OC(O)O-CH₂CHN⁺R₂]⁰ + H⁺. This must be followed by release of the oxidized TEOA to form the CO₂-bound catalyst TiO₂(e⁻)-[Re^{II}(bpy)(CO)₃CO₂]⁰, where the CO₂ carbon now coordinates to the Re center and two reducing equivalents are located on the CO₂ group. The CO₂ may be derived from the carbonate-TEOA ligand that loses TEOA and rearranges to carbon coordination. Alternatively, the entire ligand decoordinates to form the one-electron-reduced, 17-electron species TiO₂(e⁻)-[Re^I(bpy)(CO)₃]⁰ that then binds another CO₂ molecule. Both pathways end up forming the critical TiO₂(e⁻)-[Re^{II}(bpy)(CO)₃CO₂]⁰ species. On a time scale of milliseconds to seconds, electrons in the CB of TiO₂ reduce [Re^{II}(bpy)(CO)₃CO₂]⁰ to form the metalcarboxylate intermediate species TiO₂-[Re^I(bpy)(CO)₃CO₂]⁻. The metalcarboxylate intermediate can undergo a protonation (from TEOA/DMF) followed by loss of H₂O to generate TiO₂-[Re^I(bpy)(CO)₃CO]⁺.⁴² This 18-electron species must be reduced before CO is released and the starting complex is regenerated. The question is where does this final electron come from under our experimental conditions. Based on results from Kubiak and coworkers³⁵, we suggest that a small fraction of a electron equivalents, from the TiO₂ CB, could catalytically reduce the entire population of [Re^I(bpy)(CO)₃CO]⁺.

Kubiak and coworkers found that sub-stoichiometric amounts (~0.1 eqs) of reductant was sufficient to convert an entire sample of [Re^I(bpy)(CO)₃CO]⁺ to [Re^I(bpy)(CO)₃DMF]⁺ in homogeneous solution. They presented a mechanism with an electron-transfer-catalyzed ligand exchange.³⁵ Formation of TiO₂-[Re^I(bpy)(CO)₃CO]⁺ in a small amount leads to replacement of CO with solvent molecule (DMF) to form TiO₂-[Re^I(bpy)(CO)₃DMF]⁰. This complex is more reducing than the CO-complex and therefore undergoes electron transfer with TiO₂-[Re^I(bpy)(CO)₃CO]⁺ to propagate the reduction-ligand exchange process, according to the small loop presented in Scheme 2.³⁵ Finally, TiO₂-[Re^I(bpy)(CO)₃DMF]⁰ binds TEOA and CO₂ to reform the starting material, as it was before laser flash initiation. Note that the scheme does not indicate all possible charge

recombination steps and other loss pathways, which presumably make the overall quantum yield much less than 100%. The most interesting part of the proposed mechanism is that the catalyst is able to inject electrons to TiO₂ and when the catalyst becomes reduced by TEOA it can accept the electron back. This explains the redox active role of TiO₂ as an electron reservoir in TiO₂-catalyst system in presence of TEOA and CO₂.



Scheme 2, proposed photo-catalytic mechanism of attached [Re^I(bpy)(CO)₃]⁺ catalyst attached to TiO₂ surface for CO₂ reduction. The states formed on the ps-μs time scale were spectroscopically observed (above the dashed line) while the remaining species (below the dashed line) are suggested based on published mechanisms to complete a catalytic turnover (see text). For simplicity of notation we ignore the (CO)₃ groups in the catalyst chemical structure in this scheme.

CONCLUSION

We have shown that TiO₂ plays an important and active role in the photo-catalytic reduction of CO₂ by the [Re^I(bpy)(CO)₃L]⁺ catalyst in DMF with TEOA. Firstly, the electron injection from the excited catalyst to TiO₂ is followed by rapid and efficient regeneration of the Re^I center by the attached TEOA ligand. A second electron transfer, from the TEOA radical cation, leads to formation of the singly reduced [Re^I(bpy)(CO)₃L] species on the time scale of 35 ns. We propose that the increase in photocatalytic activity observed when the catalyst is bound to TiO₂, as compared to ZrO₂ or in homogeneous solution²¹, is due to the slow charge recombination and high oxidative power of the Re^{II} species after injection, as compared to the excited MLCT state on ZrO₂ or in solution, which results in a more efficient reaction with TEOA. Secondly, it seems that TiO₂ works as an electron bank that is able to accept, save and give back the electrons to the catalyst and thus to help complete the photochemical reduction of CO₂.

ASSOCIATED CONTENT

Supporting Information.

steady-state absorption, emission and IR, and complementary time-resolved IR spectroscopic data. This material is available free of charge via the Internet at <http://pubs.acs.org>.

AUTHOR INFORMATION**Corresponding Author**

*Prof. Leif Hammarström

(Leif.Hammarstrom@kemi.uu.se)

*Dr. Mohamed Abdellah

(Mohamed.Qenawy@kemi.uu.se)

Notes

The authors declare no competing financial interests.

ACKNOWLEDGMENT

The authors are grateful for funding from the Knut and Alice Wallenberg Foundation, the Swedish Energy Agency, the Swedish Research Council, the Austrian Christian Doppler Research Association (Austrian Federal Ministry of Science, Research and Economy and the National Foundation for Research, Technology and Development) and the OMV Group. Dr. Mohammad Mirmohades, Jens Föhlner and Luca D'Amario are acknowledged for their help with fs-TRIR and ns-FTIR. Prof. Sascha Ott is also acknowledged for his helpful discussion. We are dedicating this work to the soul of Prof. Ahmed Zewail.

REFERENCES

- (1) Field, C.B.; V.R. Barros, D.J. Dokken, K.J. Mach, M.D. Mastrandrea, T.E. Bilir, M. Chatterjee, K.L. Ebi, Y.O. Estrada, R.C. Genova, B. Girma, E.S. Kissel, A.N. Levy, S. MacCracken, P.R. Mastrandrea, and L.L. White (eds.), *Climate Change 2014: Impacts, Adaptation, and Vulnerability. Part A: Global and Sectoral Aspects. Contribution of Working Group II to the Fifth Assessment Report of the Intergovernmental Panel on Climate Change*, Cambridge University Press, Cambridge, United Kingdom and New York, NY, USA, **2014**.
- (2) Riplinger, C.; Sampson, M. D.; Ritzmann, A. M.; Kubiak, C. P.; Carter, E. A. *J. Am. Chem. Soc.* **2014**, *136*, 16285.
- (3) Roldan, A.; Hollingsworth, N.; Roffey, A.; Islam, H. U.; Goodall, J. B. M.; Catlow, C. R. A.; Darr, J. A.; Bras, W.; Sankar, G.; Holt, K. B.; Hogarth, G.; de Leeuw, N. H. *Chem. Commun.* **2015**, *51*, 7501.
- (4) Takeda, H.; Koizumi, H.; Okamoto, K.; Ishitani, O. *Chem. Commun.* **2014**, *50*, 1491.
- (5) Won, D.-I.; Lee, J.-S.; Ji, J.-M.; Jung, W.-J.; Son, H.-J.; Pac, C.; Kang, S. O. *J. Am. Chem. Soc.* **2015**, *137*, 13679.
- (6) Appel, A. M.; Bercaw, J. E.; Bocarsly, A. B.; Dobbek, H.; DuBois, D. L.; Dupuis, M.; Ferry, J. G.; Fujita, E.; Hille, R.; Kenis, P. J. A.; Kerfeld, C. A.; Morris, R. H.; Peden, C. H. F.; Portis, A. R.; Ragsdale, S. W.; Rauchfuss, T. B.; Reek, J. N. H.; Seefeldt, L. C.; Thauer, R. K.; Waldrop, G. L. *Chem. Rev.* **2013**, *113*, 6621.
- (7) Sahara, G.; Ishitani, O. *Inorg. Chem.* **2015**, *54*, 5096.
- (8) Morris, A. J.; Meyer, G. J.; Fujita, E. *Acc. Chem. Res.* **2009**, *42*, 1983.
- (9) Windle, C. D.; Campian, M. V.; Duhme-Klair, A.-K.; Gibson, E. A.; Perutz, R. N.; Schneider, J. *Chem. Commun.* **2012**, *48*, 8189.
- (10) Windle, C. D.; Perutz, R. N. *Coord. Chem. Rev.* **2012**, *256*, 2562.
- (11) Figueiredo, M. C.; Ledezma-Yanez, I.; Koper, M. T. M. *ACS Catal.* **2016**, *6*, 2382.
- (12) Li, C. W.; Kanan, M. W. *J. Am. Chem. Soc.* **2012**, *134*, 7231.
- (13) White, J. L.; Baruch, M. F.; Pander III, J. E.; Hu, Y.; Fortmeyer, I. C.; Park, J. E.; Zhang, T.; Liao, K.; Gu, J.; Yan, Y.; Shaw, T. W.; Abelev, E.; Bocarsly, A. B. *Chem. Rev.* **2015**, *115*, 12888.
- (14) Woolerton, T. W.; Sheard, S.; Reisner, E.; Pierce, E.; Ragsdale, S. W.; Armstrong, F. A. *J. Am. Chem. Soc.* **2010**, *132*, 2132.
- (15) Woolerton, T. W.; Sheard, S.; Pierce, E.; Ragsdale, S. W.; Armstrong, F. A. *Energy Environ. Sci.* **2011**, *4*, 2393.
- (16) Manbeck, G. F.; Muckerman, J. T.; Szalda, D. J.; Himeda, Y.; Fujita, E. *J. Phys. Chem. B* **2015**, *119*, 7457.
- (17) Agarwal, J.; Fujita, E.; Schaefer, H. F.; Muckerman, J. T. *J. Am. Chem. Soc.* **2012**, *134*, 5180.
- (18) Kumar, B.; Llorente, M.; Froehlich, J.; Dang, T.; Sathrum, A.; Kubiak, C. P. *Annu. Rev. Phys. Chem.* **2012**, *63*, 541.
- (19) Pastor, E.; Pesci, F. M.; Reynal, A.; Handoko, A. D.; Guo, M.; An, X.; Cowan, A. J.; Klug, D. R.; Durrant, J. R.; Tang, J. *Phys. Chem. Chem. Phys.* **2014**, *16*, 5922.
- (20) Hawecker, J.; Lehn, J.-M.; Ziessel, R. *J. Chem. Soc., Chem. Commun.* **1983**, 536.
- (21) Windle, C. D.; Pastor, E.; Reynal, A.; Whitwood, A. C.; Vaynzof, Y.; Durrant, J. R.; Perutz, R. N.; Reisner, E. *Chem. Eur. J.* **2015**, *21*, 3746.
- (22) She, C.; Guo, J.; Lian, T. *J. Phys. Chem. B* **2007**, *111*, 6903.
- (23) Nahhas, A. E.; Cannizzo, A.; Mourik, F. v.; Blanco-Rodríguez, A. M.; Zális, S.; Vlček, J. A.; Chergui, M. *J. Phys. Chem. A* **2010**, *114*, 6361.
- (24) El Nahhas, A.; Consani, C.; Blanco-Rodríguez, A. M.; Lancaster, K. M.; Braem, O.; Cannizzo, A.; Towrie, M.; Clark, I. P.; Zális, S.; Chergui, M.; Vlček, A. *Inorg. Chem.* **2011**, *50*, 2932.
- (25) Asbury, J. B.; Hao, E.; Wang, Y.; Lian, T. *J. Phys. Chem. B* **2000**, *104*, 11957.
- (26) Antila, L. J.; Santomauro, F. G.; Hammarstrom, L.; Fernandes, D. L. A.; Sa, J. *Chem. Commun.* **2015**, *51*, 10914.
- (27) Mirmohades, M.; Pullen, S.; Stein, M.; Maji, S.; Ott, S.; Hammarström, L.; Lomoth, R. *J. Am. Chem. Soc.* **2014**, *136*, 17366.
- (28) Mirmohades, M.; Adamska-Venkatesh, A.; Sommer, C.; Reijerse, E.; Lomoth, R.; Lubitz, W.; Hammarström, L. *J. Phys. Chem. Lett.* **2016**, *7*, 3290.
- (29) Kirgan, R. A.; Sullivan, B. P.; Rillema, D. P. In *Photochemistry and Photophysics of Coordination Compounds II*; Balzani, V., Campagna, S., Eds.; Springer Berlin Heidelberg: Berlin, Heidelberg, 2007; p 45.
- (30) Morimoto, T.; Nakajima, T.; Sawa, S.; Nakanishi, R.; Imori, D.; Ishitani, O. *J. Am. Chem. Soc.* **2013**, *135*, 16825.
- (31) Wang, Y.; Asbury, J. B.; Lian, T. *J. Phys. Chem. A* **2000**, *104*, 4291.
- (32) Anderson, N. A.; Lian, T. *Coord. Chem. Rev.* **2004**, *248*, 1231.
- (33) Anderson, N. A.; Ai, X.; Lian, T. *J. Phys. Chem. B* **2003**, *107*, 14414.
- (34) Smieja, J. M.; Kubiak, C. P. *Inorg. Chem.* **2010**, *49*, 9283.
- (35) Grice, K. A.; Gu, N. X.; Sampson, M. D.; Kubiak, C. P. *Dalton Trans.* **2013**, *42*, 8498.
- (36) Reithmeier, R.; Bruckmeier, C.; Rieger, B. *Catalysts* **2012**, *2*, 544.
- (37) Takeda, H.; Koike, K.; Inoue, H.; Ishitani, O. *J. Am. Chem. Soc.* **2008**, *130*, 2023.
- (38) Amouyal, E. *Sol. Energy Mater. Sol. Cells* **1995**, *38*, 249.
- (39) Lehn, J. M.; Sauvage, J.; GAUTHIER-VILLARS 120 BLVD SAINT-GERMAIN, 75280 PARIS, FRANCE: 1977; Vol. 1, p 449.
- (40) Kou, Y.; Nabetani, Y.; Masui, D.; Shimada, T.; Takagi, S.; Tachibana, H.; Inoue, H. *J. Am. Chem. Soc.* **2014**, *136*, 6021.
- (41) Sampson, M. D.; Froehlich, J. D.; Smieja, J. M.; Benson, E. E.; Sharp, I. D.; Kubiak, C. P. *Energy Environ. Sci.* **2013**, *6*, 3748.
- (42) Schneider, T. W.; Ertem, M. Z.; Muckerman, J. T.; Angeles-Boza, A. M. *ACS Catal.* **2016**, *6*, 5473.

Insert Table of Contents artwork here

TRIR Spectroscopy

